

This article was downloaded by:

On: 22 January 2011

Access details: *Access Details: Free Access*

Publisher *Taylor & Francis*

Informa Ltd Registered in England and Wales Registered Number: 1072954 Registered office: Mortimer House, 37-41 Mortimer Street, London W1T 3JH, UK



## The Journal of Adhesion

Publication details, including instructions for authors and subscription information:

<http://www.informaworld.com/smpp/title~content=t713453635>

### Graphite-Epoxy Composites: Effects of An Applied Interphase

J. P. Bell<sup>a</sup>; A. S. Wimolkiatisak<sup>a</sup>; H. W. Rhee<sup>a</sup>; J. Chang<sup>a</sup>; R. Joseph<sup>a</sup>; W. Kimy<sup>a</sup>; D. A. Scola<sup>a</sup>

<sup>a</sup> Polymer Science Program and Chemical Engineering Department, University of Connecticut, Storrs, CT, USA

**To cite this Article** Bell, J. P. , Wimolkiatisak, A. S. , Rhee, H. W. , Chang, J. , Joseph, R. , Kimy, W. and Scola, D. A.(1995) 'Graphite-Epoxy Composites: Effects of An Applied Interphase', The Journal of Adhesion, 53: 1, 103 – 116

**To link to this Article:** DOI: 10.1080/00218469508014374

**URL:** <http://dx.doi.org/10.1080/00218469508014374>

PLEASE SCROLL DOWN FOR ARTICLE

Full terms and conditions of use: <http://www.informaworld.com/terms-and-conditions-of-access.pdf>

This article may be used for research, teaching and private study purposes. Any substantial or systematic reproduction, re-distribution, re-selling, loan or sub-licensing, systematic supply or distribution in any form to anyone is expressly forbidden.

The publisher does not give any warranty express or implied or make any representation that the contents will be complete or accurate or up to date. The accuracy of any instructions, formulae and drug doses should be independently verified with primary sources. The publisher shall not be liable for any loss, actions, claims, proceedings, demand or costs or damages whatsoever or howsoever caused arising directly or indirectly in connection with or arising out of the use of this material.

# Graphite-Epoxy Composites: Effects of An Applied Interphase\*

J. P. BELL, A. S. WIMOLKIATISAK, H. W. RHEE, J. CHANG, R. JOSEPH,  
W. KIM and D. A. SCOLA

*Polymer Science Program and Chemical Engineering Department, University of Connecticut, Storrs, CT 06269-3136, USA*

*(Received April 16, 1994; in final form February 17, 1995)*

An applied interphase, between matrix resin and fibers in continuous fiber composites, resulted in a significant improvement in composite impact strength and fracture toughness concurrently with a moderate improvement or unchanged interlaminar shear strength. The temperature resistance of tailored interphases and composites was high. An optimum thickness was observed. The merits of such interphases and a novel means of application are discussed.

**KEYWORDS:** interlayer; interphase; graphite fibers; electropolymerization; impact strength; interlaminar shear strength; composites; graphite/epoxy.

## INTRODUCTION

The concept of using a thin, ductile interphase as a buffer between graphite fibers and glassy thermoset composite matrices, especially epoxies, has been investigated by us over the past several years. This paper will give a brief review of that work, plus some additional data.

A ductile interphase, of 0.1–0.2 microns thickness, offers several advantages: (a) the interphase can absorb interphase crack tip energy and blunt the crack tip; (b) stress concentrations resulting from thermal expansion coefficient and modulus mismatch can be relieved, and; (c) the interphase can help heal fiber surface flaws and also provide fiber protection during handling.

A general problem with graphite fiber/thermoset composites is that a compromise must usually be made between composite toughness and interlaminar shear strength.<sup>1–6</sup> There have been efforts to arrive at an optimum balance between these two properties.<sup>7</sup> Alternatively, a properly designed interphase has the possibility of providing simultaneous improvement in both toughness and interlaminar shear strength, as will be shown in this paper. Other efforts to solve this toughness-shear strength balance problem include use of more ductile thermoplastic matrices,<sup>8–11</sup> and incorporation of interpenetrating network matrices which have improved toughness

---

\* One of a Collection of papers honoring Lawrence T. Drzal, the recipient in February 1994 of *The Adhesion Society Award for Excellence in Adhesion Science, Sponsored by 3M.*

and easy processing.<sup>12-27</sup> Since epoxies are easily processed and are in dominant use, however, it is difficult to persuade designers to switch to other unproven, and often more expensive, matrix materials.

Uniform interphase coatings of controllable thickness, throughout the graphite fiber bundle, have been produced by electropolymerization of monomers directly onto the fiber surface. Details of the electropolymerization method are described elsewhere,<sup>2, 28</sup> as is the detailed characterization of the coated fibers. A brief description will be provided below.

## EXPERIMENTAL

### 1. Unidirectional Composite Preparation

Hercules AS-4 unsized fibers, in a 3000-filament bundle, were wound onto a 152 × 203 mm aluminum frame, five plies thick (approx. 20 g fibers) with light tension. The frame was inserted into an electrochemical cell for coating, as described in the next section. For control specimens, the frame was directly impregnated with matrix resin by a solvent process, as follows: 18 g of a stoichiometric mixture of methylene dianiline (MDA) curing agent and diglycidyl ether of bisphenol A (Epon 828, Shell Chemical) was mixed with 10 g acetone and the mixture was pipetted onto the fibers on the frame as uniformly as possible. The resin-impregnated fibers were then dried under vacuum for 30 min at room temperature, and at 80°C for 45 min. The prepreg was next cut into the shape of our mold (62 mm × 152 mm) and four layers, each containing 5 plies, were placed in the mold. The compression molding-curing cycle was 80°C for 30 min, without pressure, 80°C for 2 h with 14.5 mPa pressure, and 150°C for 2 h under pressure of about 16 mPa. Following this, the press heat was turned off and the samples were cooled slowly to room temperature. Pressure was used as a variable to control the fiber volume fraction. After cooling, the samples were cut into the desired test geometries. Scanning microscopic examination of composite cross sections showed very good distribution of evenly-spaced fibers, with no dry or extremely resin-rich areas. The resin-impregnation procedure for the coated fibers was the same, except that the coated fibers were cut into the shape of the mold before applying the matrix resin.

### 2. Electropolymerization Process

A process schematic is shown in Figure 1. Fibers were coated in the center cathode compartment. Polymerization conditions were as follows:

**Cathode solution:** monomer(s) (3–7% w/w), 0.05 M H<sub>2</sub>SO<sub>4</sub>, with dimethyl acetamide added as necessary to retain the monomer(s) in solution (up to 50% solvent by weight) and to swell, but not dissolve, the polymer coating.

**Anode solution:** the same composition as used in the cathode compartment, but without monomers.

**Purge:** The contents of both the anode and cathode compartments were pre-purged with nitrogen for 10 min to remove oxygen, which would react with the free radicals being formed at the cathode.

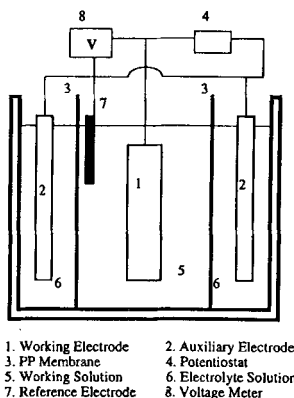


FIGURE 1 Schematic diagram of an electropolymerization cell.

Current: Held constant at  $\sim 5$ – $20$  milliamperes/g of fiber, and a SCE reference electrode voltage of  $1.3$ – $1.9$  volts.

Post-treatment: Quick rinse in a distilled water bath to remove residual monomer and/or solvent, followed by drying in a vacuum oven to complete solvent/water removal.

Additional details and procedures are available in References 2 and 28.

A continuous process for coating graphite fiber continuous strands was also developed, and is described elsewhere.<sup>2, 29</sup> The data for the coated fibers and composites described in this paper were obtained from the batch process, however.

### 3. Coating Thickness Measurements

The interphase thickness was controlled by varying the electropolymerization time. The interphase thickness increased linearly with electropolymerization time. The interphase thickness was determined from the interphase weight gain on the graphite fibers. Knowing the weight gain, fiber diameter ( $7.14$  microns), density of the fiber ( $1.8$  g/cc), and density of the interphase, the thickness can be calculated.

$$\text{Thickness} = R_c - R_f$$

$$R_c = \left[ \left( \frac{W \times \rho_f \times R_f^2}{\rho_i} \right) + R_f^2 \right]^{0.5}$$

$W$  = weight gain in gms resin/gm of fiber  
 $R_f$  = fiber radius, cm  
 $R_c$  = (fiber radius + coating thickness), cm  
 $\rho_f$  = fiber density, gms/cc  
 $\rho_i$  = interphase density, gms/cc

The above equation yielded an average interphase thickness value. It is derived based on the following assumptions: a) the interphase is coated uniformly on the fiber surface, b) the density of the interphase material is the same whether it is at the interphase or as a bulk polymer.

#### 4. Normalization of IMPR, ILSS and $G_{1C}$ Data

The impact strength (IMPR) and interlaminar shear strength (ILSS) of the control composites strongly depend upon the fiber volume percent,  $V_f$ . Both properties increase with increasing  $V_f$  in a manner that can be fitted well by a straight line over the range  $V_f = 50\text{--}70\%$ .<sup>1,2</sup> On the other hand,  $G_{1C}$  is much less dependent upon  $V_f$ .<sup>38</sup> The three properties may be fitted by the following equations for the control systems reported here.<sup>38</sup>

$$\text{IMPR} = 46.53 + 0.45 V_f$$

$$\text{ILSS} = 31.03 + 0.788 V_f$$

$$G_{1C} = 339 + 1.15 V_f$$

where IMPR, ILSS,  $G_{1C}$  and  $V_f$  have units of  $\text{kJ/m}^2$ , MPa,  $\text{J/m}^2$  and %, respectively. These equations were then used to normalize the  $V_f$  effect so that properties with and without the interphase could be compared at the same  $V_f$ . The normalization was done by taking the ratio of the property of the interphase composite over the control composite at the same fiber volume fraction. The values for the controls are readily calculated from the above equations, and the values for the interphase composites are obtained by multiplying the control value by the normalized ratio shown as the ordinate on Figures 3, 4 and 7–11. As an example, an interphase composite at  $V_f = 50\%$  gave an IMPR of  $80 \text{ kJ/m}^2$ . By substituting 50% into the top equation above, one finds a value for the control of  $69 \text{ kJ/m}^2$ . The normalized value is then  $80/69$  or 1.16, which could be plotted on Figure 3a. In most instances,  $V_f$  of the interphase composites was close to 60%.

## RESULTS AND DISCUSSION

### 1. Early Feasibility Studies

Early work by the authors and others established that a variety of acrylic monomers could be electropolymerized and electrocopolymerized onto graphite fibers in a controlled manner.<sup>30–34</sup> Monomers polymerized either singly or in pairs included acrylonitrile, methyl acrylate, methyl methacrylate, glycidyl acrylate, acrylic acid and a few other vinyl group-containing compounds. All of the polymers produced from these monomers have glass transition temperatures below the desired operating temperatures ( $180\text{--}200^\circ\text{C}$ ) for many composites, and would be expected to flow above their glass transition. In the later part of this work, to be discussed below, polymers with  $T_g$ 's  $> 220\text{--}240^\circ\text{C}$  were investigated. However, the early low  $T_g$  acrylic and vinyl interphase work provided information about many important experimental and property parameters.<sup>29, 31, 33, 37, 38</sup>

### 2. Coating Uniformity

To determine the variability of a typical interphase thickness from the electropolymerization process, a frame was sampled at the surface locations shown on Figure 2. In

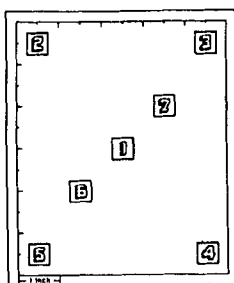


FIGURE 2 Sampling locations in continuing uniformity experiments.

TABLE Ia  
Char residue as a function of composition

Feed Composition (Volume)	Polymer Composition (mole)	Char Residue, %
GA/MA = 4/0	GA/MA = 100.0/0.0	—
1/3	13.6/86.4	3.5
1/15	8.0/92.0	2.5

TABLE Ib  
Determination of coating uniformity at different locations

Position	Weight Loss, %	Yield <sub>TGA</sub> , %	Yield <sub>weight</sub> , %
1	14.75	15.34	—
2	14.75	15.34	—
3	14.0	14.56	—
4	13.25	13.78	—
5	14.0	14.56	—
Average	14.15	14.72	15.14

Yield<sub>TGA</sub>: weight gain calculated from weight loss dataYield<sub>weight</sub>: weight gain obtained from weight measurement

separate experiments, the char residue was determined for polymer samples containing different ratios of glycidyl acrylate to methyl acrylate. Thermogravimetric analyses (TGA) to 900°C gave a weight loss equal to the polymer weight minus the remaining char weight (Table Ia). By this method, it was possible to determine the amounts of polymer that had been coated onto the fiber samples, which were approximately 20 mg in weight. The results of the measurements at different locations are shown in Table Ib. The uncorrected TGA weight loss values and the corresponding char-corrected yield values both vary by about  $\pm 5\%$ . These results are in agreement with the overall gain in weight of the sample, shown in the column at the right side of the Table.

To determine variability as a function of depth, cross-section “plugs” were taken out of the sample at locations 6 and 7, and TGA measurements were made at inner (center of the H-frame), middle and outer locations. As shown in Table II, the variation was

TABLE II  
Determination of coating uniformity as a function

Position	Weight Loss, % (Position 6)	Weight loss (Position 7)	Average, %
Inner	14.7	14.9	14.8
Middle	14.8	15.6	15.2
Outer	15.3	14.5	14.9
Average	14.9	15.0	15.0

small. Both these data and the data of the previous paragraph show that the amount of coating is fairly uniform throughout the frame.

Of course, different results may be obtained for different fiber tension, different numbers of plies, or by using 12000-filament bundles as opposed to the 3000-filament bundles of this work. The molecular size and speed of polymerization of the comonomers may affect the results, as well as mass transfer from the cathode solution. The cathode solution was recirculated through an external tubing peristaltic pump in these experiments.<sup>2</sup>

### 3. Bonding Between Interphase and Matrix

The importance of excellent bonding between the interphase and the matrix polymer is illustrated by comparison of Figures 3 and 4. In Figure 3 the interphase is comprised of a glycidyl acrylate polymer (PGA interphase) which is reactive with the amine-containing epoxy matrix. In Figure 4 the interphase is comprised of an 8 mol% glycidyl acrylate/92 mol% methyl acrylate copolymer with little reactivity toward the amine-

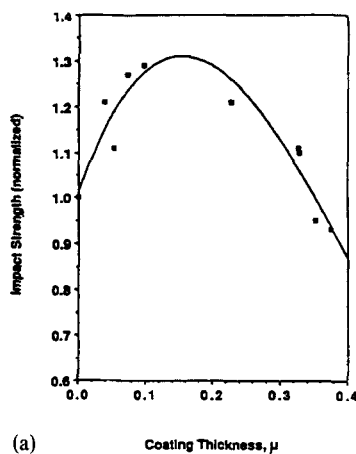


FIGURE 3a Impact strength vs. coating thickness of composites with PGA interlayer.

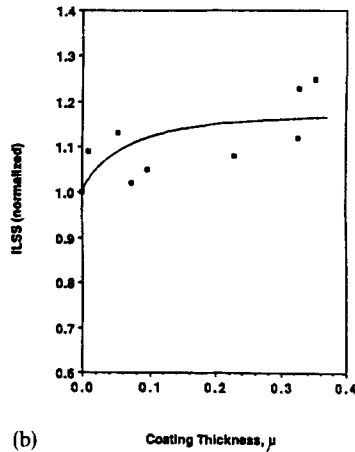


FIGURE 3b ILSS vs. coating thickness of composites with PGA interlayer.

containing epoxy. Clearly the matrix-reactive system (Fig. 3) resulted in a significant increase in interlaminar shear strength (ILSS) and impact strength (IMPR) (same vol% fibers), relative to the much-less-reactive 8/92 mole % mixture (Fig. 4). Scanning Electron Microscopic examination revealed that failure occurred at the fiber/interphase junction for the 100 mol% glycidyl acrylate system and at the interphase/epoxy junction for the 8/92 GA/MA mole % system.

#### 4. Optimum Interphase Thickness

The data in Figures 3a and 5 show that a maximum improvement in impact strength is achieved at about 0.12 to 0.16 microns thickness. The same optimum value of 0.16 microns was also found for a completely different polymer system (3-car-

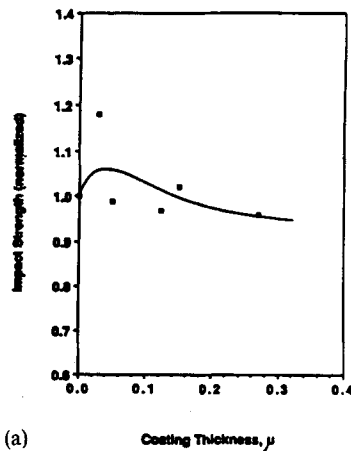


FIGURE 4a Impact strength vs. coating thickness of composites with GA/MA = 1/15 interlayer.



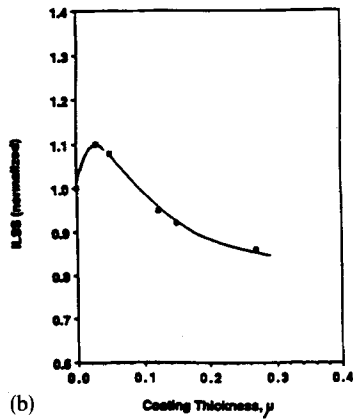


FIGURE 4b ILSS vs. coating thickness of composites with GA/MA = 1/15 interlayer.

boxyphenyl maleimide/styrene, to be discussed below).<sup>36</sup> A series of acrylonitrile/methyl acrylate copolymers of monomer ratios such that  $T_g = 18^\circ\text{C}$ ,  $23^\circ\text{C}$  and  $39^\circ\text{C}$  was tested. All three showed impact strength improvement, but the  $18^\circ\text{C}$  sample showed a rapid drop in both interlaminar shear and impact strengths when tested above the optimum thickness.<sup>1</sup> The Mode I crack opening fracture toughness of acrylic-coated graphite fiber composites showed an improvement of approximately 50% relative to controls.<sup>37</sup>

As a possible explanation of the thickness dependence, at thicknesses lower than the optimum value a fully-developed crack tip region is not easily formed because of the constraints from the graphite and nearby matrix surfaces. At thicknesses greater than the optimum, the fracture toughness of the bulk interphase polymer becomes limiting. This fracture toughness of the interphase may be lower than that of the bulk epoxy.

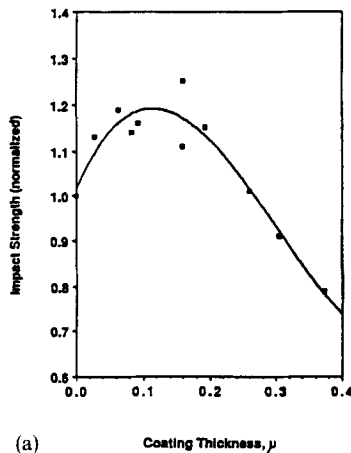


FIGURE 5a Impact strength vs. coating thickness of composites with GA/MA = 1/3 interlayer.

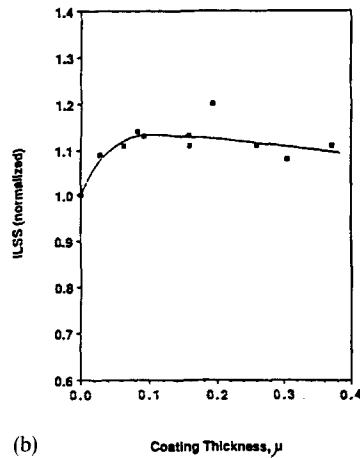


FIGURE 5b ILSS vs. coating thickness of composites with GA/MA = 1/3 interlayer.

Also, if the coating is too thick, the fibers may stick together, forming bundles which can reduce resin distribution efficiency and reduce the mechanical properties.

### 5. The Effect of Temperature Upon Interphase/Composite Properties

A reasonable question is how the relatively low  $T_g$  acrylic interphases would perform in a high use temperature environment. Many aerospace applications require performance at 180°C or higher. To investigate this point, we investigated the “apparent or effective interfacial shear strength” ( $\tau_e$ ) from single fiber fracture tests<sup>38</sup> as a function of temperature. Since the equations used to calculate interfacial shear strength assume

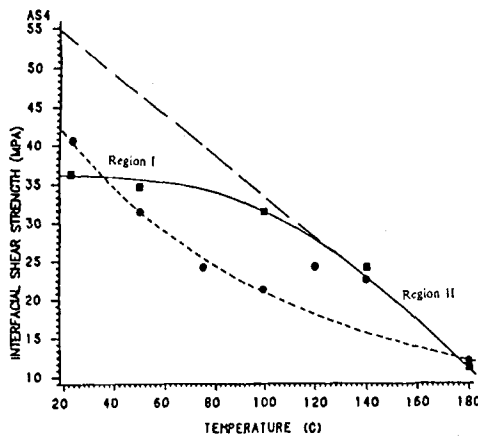


FIGURE 6  $\tau_e$  as a function of temperature. Solid line is for control sample, dashed line is for GA/AN coated sample.

plastic deformation of the matrix, they are not strictly applicable in the low temperature, elastic region; hence, the term “apparent or effective interfacial shear strength”,  $\tau_e$ . The results are shown in Figure 6, with results from an epoxy/graphite control composite of the same volume fraction. The data for the control can be separated into two regions. The constancy of  $\tau_e$  with temperature in region I infers that interfacial failure limits  $\tau_e$  up to a temperature of approximately 120°C. Above this temperature, the failure curve approximates that of the pure matrix, as indicated by matrix tensile strength-temperature data (Fig. 7). The sample containing the glycidyl acrylate/acrylonitrile (2:1 vol. ratio, GA/AN) interphase has higher  $\tau_e$  than the control at room temperature, but when the  $T_g$  of the interphase is exceeded, the  $\tau_e$  drops dramatically. For satisfactory performance, the interphase must clearly either have a high  $T_g$ , or be crosslinked such that flow cannot occur. For this reason, our interphase research emphasis was changed to the high  $T_g$  polymers discussed in the next section.

## 6. High $T_g$ Thermoplastic Interphase

Consideration was given to monomers that can be readily polymerized by a free radical mechanism, yet yield high  $T_g$  polymers. While the electropolymerization process may be applicable to other than a free radical mechanism, useful high  $T_g$ , high molecular weight polymers have not yet been demonstrated, to the best of our knowledge. We chose to retain the free radical mechanism and selected substituted maleimides for investigation based upon their known high  $T_g$  values. 3-carboxyphenyl maleimide (3-CMI), when copolymerized with styrene, (3-CMI-S) in a standard solution process, was known to form an alternating copolymer with good temperature resistance.<sup>39-47</sup> It was found in our early tests that the monomers could be used in our process with about 50% solvent mixed with water to retain them in solution, whereas earlier work was almost entirely nonaqueous. The polymer coatings could be produced in any thickness up to that required for the coating to become the entire matrix. The  $T_g$  of 220°C was satisfactory, and weight loss by thermogravimetric analysis was not observed until 400–450°C.

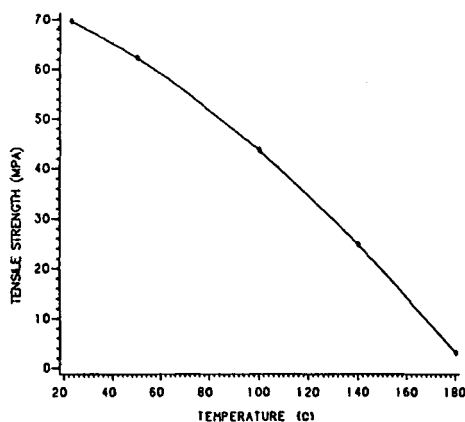


FIGURE 7 Tensile strength vs. temperature for EPON828-MDA.

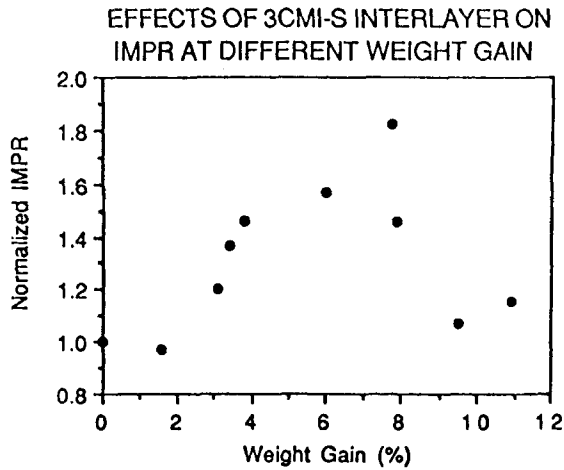


FIGURE 8  $V_f$ -normalized impact resistance vs. 3CMI-S weight gain.

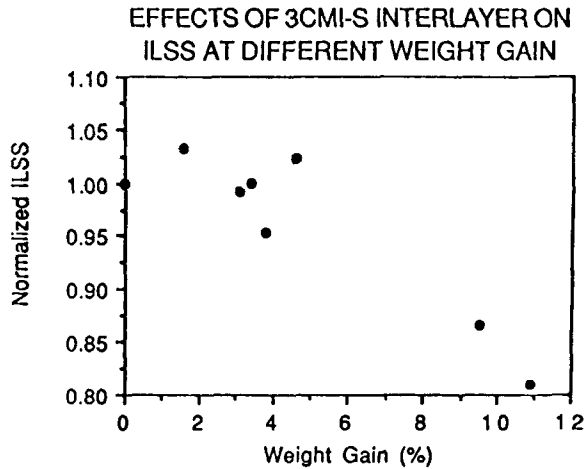


FIGURE 9  $V_f$ -normalized interlaminar shear strength vs. 3CMI-S weight gain.

Impact strength (IMPR) and interlaminar shear strength (ILSS) data are presented in Figures 8 and 9. The data have again been normalized to 60 vol. % fiber content (actual samples were only slightly different from this value), and are presented as the ratio of the interphase composite property to the control composite property, *i.e.*, the control is presented as 1.0. A weight gain of six percent corresponds to 0.15 microns coating thickness. An improvement in IMPR of about 60 percent at the optimum coating thickness, with essentially the same ILSS value, is observed (Fig. 8).

To evaluate toughness at much lower strain rates, the fracture toughness values  $G_{Ic}$  and  $G_{Ic\ initial}$  were evaluated, using double cantilever beam specimens in Mode I (crack opening) experiments. These experiments are extensive and are described in detail

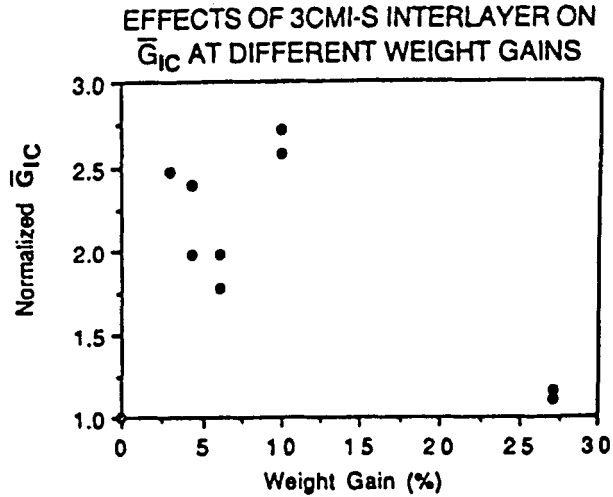


FIGURE 10  $V_f$ -normalized average  $G_{IC}$  vs. 3CMI-S weight gain.

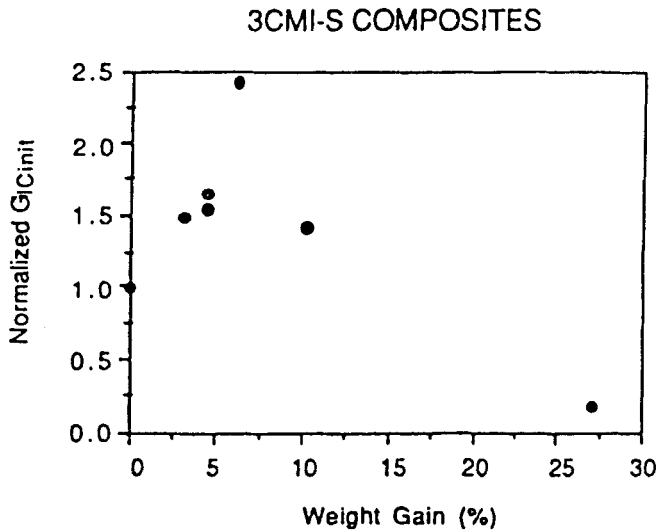


FIGURE 11  $V_f$ -normalized initial  $G_{IC}$  vs. 3CMI-S weight gain.

elsewhere.<sup>36</sup>  $G_{IC}$  often gives somewhat higher results than  $G_{IC\ initial}$  because of fiber bridging from one ply to another as the crack extends.  $G_{IC\ initial}$  involves only the first few data points on a compliance vs. crack length plot, and is indicative of the level of toughness before bridging becomes important.

The  $G_{IC}$  and  $G_{IC\ initial}$  results were normalized with respect to fiber volume fraction and are presented as a ratio to control composites at the same fiber content, but

without an interphase. The results are shown in Figures 10 and 11. While there is considerable scatter in the Figure 10 data (but note the data points at the lower right corner), the data compare favorably with those from the impact measurements and from the acrylic polymer systems. The  $G_{Ic\ initial}$  data of Figure 10 show a maximum in the 5% weight gain area ( $0.15\ \mu$ ). For both  $G_{Ic\ initial}$  and  $G_{Ic}$  the interphase advantage is lost at very high thicknesses, as was true for IMPR and ILSS.

## CONCLUSIONS

Thin interphase polymers coated on graphite fibers generate improvements in impact resistance and fracture toughness of graphite fiber/epoxy matrix composites, in the range of 30–100%. Interlaminar shear strength is not sacrificed in this process, contrary to many other impact strength improvement systems. There is an optimum interphase thickness of approximately  $0.15\ \mu$ , for both acrylic and high  $T_g$  substituted maleimide/styrene systems. Low  $T_g$  interphase polymers, unless highly crosslinked to prevent flow, are not mechanically effective at high use temperatures. Interfacial bonding between an interphase and the matrix polymer was found to be effective in our systems. Overall, electropolymerized interphase polymers offer an attractive possibility for improvement in the toughness of thermoset/graphite fiber composites.

## Acknowledgements

This work was supported by the National Science Foundation (Grant No. CPE-841280).

## References

1. J. Chang, Ph.D. Thesis, Univ. of Conn., Storrs, CT (1986).
2. H. W. Rhee, Ph.D. Thesis, Univ. of Conn., Storrs, CT (1987).
3. R. V. Subramanian and J. J. Jakubowski, *Polym. Eng. & Sci.*, **18** (7), 590–600 (1978).
4. R. V. Subramanian, V. Sundaram and A. K. Patel, *Proc. 33rd SPI RP/C Conf.*, Sec. 20-F (1978).
5. R. V. Subramanian and A. S. Crasto, *Polym. Compos.* **7**(4), 201–218 (1986).
6. B. D. Agarwal and L. J. Broutman, *Analysis and Performance of Fiber Composites* (Wiley, New York, 1980).
7. A. G. Atkins, *J. Mater. Sci.* **10**, 819 (1975).
8. "Panel Discussion on: Thermoplastics Vs. Thermosets in Advanced Composites", *Polym. Compos.*, **8**(6), 437 (1987).
9. D. M. Carlin, *Proc. 47th SPE Ann. Tech. Conf.*, Vol. XXXV, May 1–4, p. 1447 (1989).
10. U. Gaur, G. Desio and B. Miller, *Proc. 47th SPE Ann. Tech. Conf.*, Vol. XXXV, May 1–4, p. 1513 (1989).
11. A. Lustiger, *Proc. 47th SPE Ann. Tech. Conf.*, Vol. XXXV, May 1–4, p. 1493 (1989).
12. R. Pater and C. Morgan, *Proc. 46th SPE Ann. Tech. Conf.*, Vol. XXIV, April 18–21, p. 1639 (1988).
13. R. Pater, *Proc. 47th SPE Ann. Tech. Conf.*, Vol. **35**, May 1–4, p. 1434 (1989).
14. A. O. Hanky and T. L. St. Clair, *SAMPE J.*, **21** (4), 40 (1985).
15. A. H. Egli, L. L. King and T. L. St. Clair, *Proc. 18th Nat'l SAMPE Tech. Conf.*, Vol. **18**, p. 440 (1986).
16. T. L. St. Clair, *ACS Interdisciplinary Symp. on Recent Advances in Polyimides and Other High Temp. Polym.*, Reno, NV, July 13–16 (1987).
17. H. Zeng and K. Mai, *Macromol. Chem.* **187**, 1787 (1986).
18. Y. Yamamoto, S. Satoh and S. Etoh, *SAMPE J.*, **21**(4), 6 (1985).
19. P. A. Steiner, J. M. Browne, M. T. Blair and J. M. McKillen, *SAMPE J.*, **23** (2), 8 (1987).
20. T. Pascal, R. Mercier and B. Sillion, *Proc. 3rd Inter. Conf. on Polyimides*, Ellenville, NY, November 2–4 (1988).

21. S. Das, B. DeBona and D. C. Prevorsek, *Proc. SPE Regional Tech. Conf.*, Los Angeles, CA, November 15–17 (1988).
22. M. S. Sefton, P. T. McGrail, J. A. Peacock, S. P. Wilkinson, R. A. Crick, M. Davies and G. Almen, *Proc. 19th Nat'l SAMPE Tech. Conf.*, Vol. 19, p. 700 (1987).
23. R. S. Rahgava, *J. Polym. Sci., Part B, Polym. Phys.*, **26**, 65 (1988).
24. R. D. Vannucci and K. J. Bowles, *Proc. 17th Nat'l SAMPE Tech. Conf.*, Vol. 17, p. 352 (1985).
25. R. H. Pater, *Proc. SPE Regional Tech. Conf.*, Los Angeles, CA, November 15–17, p. 273 (1988).
26. P. Delvigs, *Polym. Compos.*, **7** (2), 101 (1986).
27. R. H. Pater, *SAMPE J.*, **26** (5), 19 (1990).
28. J. Iroh, J. P. Bell and D. A. Scola, *J. Appl. Polym. Sci.*, **41**, 735 (1990); *Proc. SPE's RETEC*, November 14–17, Los Angeles, CA (1988).
29. Wonho Kim, M.S. Thesis, Univ. of Conn., Storrs, CT (1989).
30. J. P. Bell, J. Chang, H. W. Rhee and R. Joseph, *Polym. Compos.*, **8** (1), 46 (1987).
31. J. Chang, J. P. Bell and S. Shkolnik, *J. Appl. Polym. Sci.*, **34**, 2105 (1987).
32. A. S. Crasto, S. H. Owen and R. V. Subramanian, *Polym. Compos.*, **9** (1), 78 (1988).
33. J. P. Bell, J. Iroh, W. Kim and D. Scola, *Proc. 47th SPE Ann. Tech. Conf.*, Vol. XXXV, May 1–4, p. 565 (1989).
34. R. V. Subramanian, *Adv. Polym. Sci.*, **33**, 33 (1979).
35. H. W. Rhee and J. P. Bell, *Polymer Composites*, **12**, 213–225 (1991).
36. A. S. Wimolkiatisak and J. P. Bell, *J. Appl. Polymer Sci.*, **46**, 1899–1914 (1992).
37. R. Joseph, J. P. Bell and H. W. Rhee, *Polym. Eng. Sci.*, **28** (9), 605 (1988).
38. S. Wimolkiatisak, Ph.D. Thesis, Univ. of Conn., Storrs, CT (1990); A. S. Wimolkiatisak and J. P. Bell, *Polym. Compos.*, **10** (3), 162 (1989).
39. T. Kagiya, M. Izu and K. Fukui, *J. Polym. Sci., Part B*, **4**, 387 (1966).
40. T. Kagiya, M. Izu, S. Kawai and K. Fukui, *J. Polym. Sci., Part A-1*, **5**, 1415 (1967).
41. J. O'Donnell and R. D. Sothman, *J. Polym. Sci., Part B*, **7**, 129 (1968).
42. Z. Florjanczyk and W. Krawiec, *Makromol. Chem.*, **190**, 2141–2147 (1989).
43. T. M. Barrales-Rsenda, J. I. Gonzalez de la Campa and J. Gonzalez Ramos, *J. Macromol. Sci. Chem.*, **A11** (2), 267–286 (1977).
44. M. W. Sabaa, M. G. Mikhael, A. A. Yassin and M. Z. Elsabee, *Die Angew Makromol. Chem.*, **139**, 95 (1986).
45. M. E. Elsabee, M. G. Mikhael, M. W. Sabaa and A. A. Yassin, *Die Angew Makromol. Chem.*, **157**, 43–57 (1988).
46. K. Hayashi and G. Smets, *J. Polym. Sci.*, **37**, 275 (1958).
47. N. G. Gaylord, *J. Macromol. Sci., Rev. Macromol. Chem.*, **13**, 235 (1975).